EUROPEAN JOURNAL OF PURE AND APPLIED MATHEMATICS
2025, Vol. 18, Issue 4, Article Number 6364
ISSN 1307-5543 – ejpam.com
Published by New York Business Global

Modeling of Eye Infection Transmitting by Conjunctivitis Adenovirus: Deterministic and Stochastic Approach

Rahim ud Din[1,*], Naveed Ahmad[2], Sadique Ahmad[3], Puntani Pongsumpun[1]

[1] *Department of Mathematics, School of Science, King Mongkut's Institute of Technology Ladkrabang, Bangkok, Thailand*
[2] *EIAS Data Science and BlockChain Lab, CCIS, Prince Sultan University, Riyadh 11586, Saudi Arabia*
[3] *Department of Computer Science CCIS, Prince Sultan University, Riyadh 11586, Saudi Arabia*

Abstract. This study develops a mathematical model to investigate the early diagnosis and treatment of conjunctivitis caused by adenovirus, incorporating both deterministic and stochastic approaches to capture disease dynamics. The model's fundamental properties, including boundedness and uniqueness, are analyzed to ensure reliability, and equilibrium points are established for the deterministic framework. The basic reproduction number is derived and subjected to sensitivity analysis to evaluate how key parameters influence the spread of infection. Numerical simulations, conducted using a nonstandard finite difference (NSFD) scheme for the deterministic model and stochastic methods for the probabilistic model, reveal that individuals with strong immune systems can recover without medical intervention, highlighting the critical role of immune strength in controlling disease transmission. These findings contribute to a deeper understanding of conjunctivitis dynamics and provide valuable insights for designing effective control strategies based on early diagnosis and treatment.

2020 Mathematics Subject Classifications: 92B05, 92D30, 93A30
Key Words and Phrases: Eye infection, adenovirus, sensitivity analysis, SITR model, NSFD scheme, stochastic model

1. Introduction

Over the past few decades, the field of biological research has expanded considerably, and this growth is expected to continue with ongoing technological advancements. Mathematicians have played a key role in driving progress, contributing significant developments

*Corresponding author.
DOI: https://doi.org/10.29020/nybg.ejpam.v18i4.6364

Email addresses: 67056116@kmitl.ac.th (R. ud Din),
Nahmed@psu.edu.sa (N. Ahmad),
saahmad@psu.edu.sa (S. Ahmad), puntani.po@kmitl.ac.th (P. Pongsumpun)

that provide lasting benefits to society [1]. Mathematics has not only advanced the natural sciences but also holds great potential to transform biological research. Through mathematical modeling, biology gains valuable tools to interpret and analyze its inherent complexity. Moreover, recent progress in computer algebra systems has made it easier to address complex mathematical problems [2], enabling researchers to concentrate more on the study of mathematical biology rather than on technical problem-solving.

In recent years, there has been growing interest in the mathematical modeling of biological, physical, and epidemiological phenomena. This surge is largely due to the ability of mathematical models to account for numerous influencing factors. Mathematical biology, in particular, has attracted significant attention from researchers in areas such as body fluid dynamics, human growth modeling, infectious disease modeling, and related fields [3–5]. The widespread application of mathematical models has deepened our understanding of the complex nature of biological processes by shedding light on fundamental concepts. In the context of infectious diseases, mathematical modeling plays a vital role in identifying threshold parameters, clarifying transmission patterns, and formulating effective management strategies [6]. Moreover, by offering practical insights into treatment, mathematical models have proven valuable in both the prevention and control of infectious diseases, serving as a powerful tool in the fight against viral outbreaks [7].

Conjunctivitis, commonly known as "pink eye" or "bloodshot eyes," is an infection of the conjunctive the thin tissue covering the white part of the eye and the inner surface of the eyelid. It is a highly contagious condition that may be caused by bacteria, viruses, or allergic reactions, all of which can trigger inflammation. Conjunctivitis occurs in several forms; for instance, allergic conjunctivitis is often caused by seasonal exposure to antigens or irritants such as house dust mites, pollen, animal dander, and contact lenses [8, 9]. Transmission typically occurs when a susceptible individual comes into direct contact with an infected person or with contaminated objects, such as foreign particles that enter the eyes, or through exposure to fluids discharged from the conjunctiva or the upper respiratory tract of an infected individual. Furthermore, studies suggest a direct association between parental chlamydial or gonococcal infections and the risk of transmission to infants. This work focuses on a viral form of the disease known as acute hemorrhagic conjunctivitis (AHC). The incubation period of AHC ranges from one to three days, after which symptoms such as photophobia, sore throat, tearing, eye discomfort, and swelling may develop, often accompanied by ocular discharge [10]. Effective strategies to prevent the spread of conjunctivitis include the use of antibiotic eye drops, maintaining proper hygiene, isolating infected individuals, and allowing the viral infection to resolve naturally, which typically occurs within two to three weeks. The disease is more prevalent in tropical regions [11, 12] and is commonly observed during the rainy season, when humid conditions favor its transmission [13]. High occurrence rates have been reported in tropical areas such as Thailand [14, 15]. Isolation of affected individuals is strongly recommended to limit the spread of infection [16]. Beyond reducing transmission, home isolation also facilitates recovery while minimizing both the number and duration of infectious contacts [17]. Notable contributions to this field include the studies reported in [16, 18, 19].

Furthermore, conjunctivitis most commonly emerges during the rainy season, when high

Figure 1: Different kinds of eye infection image.

humidity creates favorable conditions for viral transmission [20]. The disease is frequently reported in tropical regions such as Thailand [21, 22]. Isolating affected individuals is strongly recommended to curb its spread. Allowing patients to take leave from work and remain in home isolation not only supports faster recovery but also reduces both the frequency and intensity of potential infectious contacts [23]. In Figure 2, we present the different types of eye infections.

We develop a mathematical model to study the dynamics of eye infections by dividing the total population into four compartments: $\mathcal{S}$ (susceptible), $\mathcal{I}$ (infected), $\mathcal{T}$ (under treatment), and $\mathcal{R}$ (recovered). The model incorporates a saturated incidence rate to describe the transmission of infection. For the deterministic framework, local stability is analyzed, and the basic reproduction number is derived using the next-generation matrix approach. Numerical simulations of the deterministic model are carried out using the NSFD scheme. For the stochastic model, properties such as exactness, uniqueness, the basic reproduction number, stability, and numerical simulations are discussed in subsequent sections.

1.1. Model Formulation

In this section of our work, we develop model for the Conjunctivitis virus. The whole population are divide into four compartments, in which $\mathcal{S}$ stand for susceptible people, $\mathcal{I}$

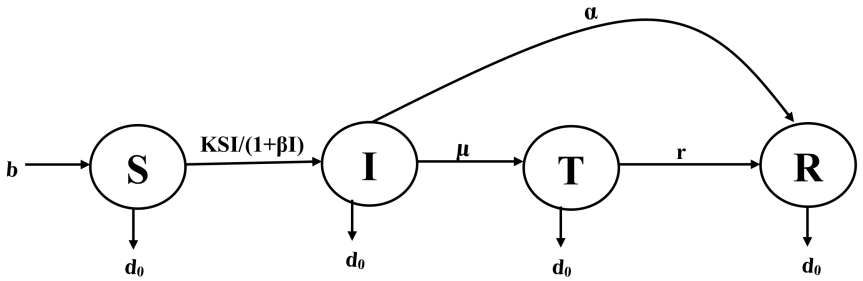

Figure 2: Representation of the model schematically (1).

Parameters	Physical Meaning
$\mathcal{S}$	Susceptible population
$\mathcal{I}$	Infected population
$\mathcal{T}$	Under treatment population
$\mathcal{R}$	Recovered population
b	Birth rate
K	Transmission rate
β	Saturation constant
α	Recovery without medication
μ	medication rate
d_0	Natural death rate
r	Recovery rate of under treatment populations

Table 1: The model (1) describes and specifies the system's parameters.

for infected people, $\mathcal{T}$ for under treatment, and $\mathcal{R}$ represent recovered populations.

$$\begin{aligned}
\frac{d\mathcal{S}}{dt} &= b - \frac{K\mathcal{S}\mathcal{I}}{1+\beta\mathcal{I}} - d_0\mathcal{S},\\
\frac{d\mathcal{I}}{dt} &= \frac{K\mathcal{S}\mathcal{I}}{1+\beta\mathcal{I}} - (\alpha+\mu+d_0)\mathcal{I},\\
\frac{d\mathcal{T}}{dt} &= \mu\mathcal{I} - (r+d_0)\mathcal{T},\\
\frac{d\mathcal{R}}{dt} &= r\mathcal{T} + \alpha\mathcal{I} - d_0\mathcal{R}.
\end{aligned} \tag{1}$$

A flowchart for the above system (1) are represented in figure (2), which shows how the community dynamics of different compartments have evolved over time.

The following table, 1.1, contains the parameters utilized in the algorithm (1) and their actual meaning.
Components in the model (1) and how they vary from one another are also given in .

2. Uniqueness and Existence

We look for the existence and uniqueness of the system (1). In order to attained this, the system (1) is described by

$$\begin{aligned} \mathcal{S}^{'} &= h_1\left(t, \mathcal{S}, \mathcal{I}, \mathcal{T}, \mathcal{R}\right), \\ \mathcal{I}^{'} &= h_2\left(t, \mathcal{S}, \mathcal{I}, \mathcal{T}, \mathcal{R}\right), \\ \mathcal{T}^{'} &= h_3\left(t, \mathcal{S}, \mathcal{I}, \mathcal{T}, \mathcal{R}\right), \\ \mathcal{R}^{'} &= h_4\left(t, \mathcal{S}, \mathcal{I}, \mathcal{T}, \mathcal{R}\right). \end{aligned} \tag{2}$$

Norm is define as

$$||\chi||_{\infty} = \sup_{t \in x}. \tag{3}$$

where $x \in [0, t]$. We assumed that for every t, $\mathcal{S}$, $\mathcal{I}$, $\mathcal{T}$, and $\mathcal{R}$ are limited in $[0, t]$ and that for each t that belongs to $[0, t]$, there exist $k_1, k_2, k_3,$, and k_4, such that

$$\begin{aligned} ||\mathcal{S}||_{\infty} &< k_1, \\ ||\mathcal{I}||_{\infty} &< k_2, \\ ||\mathcal{T}||_{\infty} &< k_3, \\ ||\mathcal{R}||_{\infty} &< k_4. \end{aligned}$$

Now, we have to prove (2) is bonded

$$\begin{aligned} |h_1\left(t, \mathcal{S}, \mathcal{I}, \mathcal{T}, \mathcal{R}\right)| &= |b - \frac{K\mathcal{S}\mathcal{I}}{1 + \beta\mathcal{I}} - d_0\mathcal{S}| \\ &\leq b + \frac{K|\mathcal{S}||\mathcal{I}|}{1 + \beta|\mathcal{I}|} + d_0|\mathcal{S}| \\ &\leq b + \frac{K}{1 + \beta k_2} k_1 k_2 + d_0 k_1 < \infty. \end{aligned} \tag{4}$$

where $t \in [0, t] = M$. Additionally, using the same process, we have

$$\begin{aligned} |h_2\left(t, \mathcal{S}, \mathcal{I}, \mathcal{T}, \mathcal{R}\right)| &= |\frac{K\mathcal{S}\mathcal{I}}{1 + \beta\mathcal{I}} - (\alpha + \mu + d_0)\mathcal{I}| \\ &\leq \frac{K}{1 + \beta k_2} k_1 k_2 + (\alpha + \mu + d_0) k_2 < \infty. \end{aligned} \tag{5}$$

$$\begin{aligned} |h_3\left(t, \mathcal{S}, \mathcal{I}, \mathcal{T}, \mathcal{R}\right)| &= |\mu\mathcal{I} - (r + d_0)\mathcal{T}| \\ &\leq \mu k_2 + (r + d_0) k_3 < \infty. \end{aligned} \tag{6}$$

$$\begin{aligned} |h_4\left(t, \mathcal{S}, \mathcal{I}, \mathcal{T}, \mathcal{R}\right)| &= |r\mathcal{T} + \alpha\mathcal{I} - d_0\mathcal{R}| \\ &\leq r k_3 + \alpha k_2 + (d_0) k_4 < \infty. \end{aligned} \tag{7}$$

Thus $\mathcal{S}, \mathcal{I}, \mathcal{T}$ and $\mathcal{R}$ are bounded and there exist L_1, L_2, L_3 and L_4 such that

$$\begin{aligned}
&\sup_M |h_1(t, \mathcal{S}, \mathcal{I}, \mathcal{T}, \mathcal{R})| < L_1,\\
&\sup_M |h_2(t, \mathcal{S}, \mathcal{I}, \mathcal{T}, \mathcal{R})| < L_2,\\
&\sup_M |h_3(t, \mathcal{S}, \mathcal{I}, \mathcal{T}, \mathcal{R})| < L_3,\\
&\sup_M |h_4(t, \mathcal{S}, \mathcal{I}, \mathcal{T}, \mathcal{R})| < L_4.
\end{aligned}$$

Next, we have to prove

$$\begin{aligned}
|h_1(t, \mathcal{S}_1, \mathcal{I}, \mathcal{T}, \mathcal{R}) - h_1(t, \mathcal{S}_2, \mathcal{I}, \mathcal{T}, \mathcal{R})| &= |b - \frac{K\mathcal{S}_1\mathcal{I}}{1+\beta\mathcal{I}} - d_0\mathcal{S}_1 - b - \frac{K\mathcal{S}_2\mathcal{I}}{1+\beta\mathcal{I}} - d_0\mathcal{S}_2|\\
&< (\frac{K\mathcal{I}}{1+\beta\mathcal{I}} + d_0)|\mathcal{S}_1 - \mathcal{S}_2|\\
&< k_1|\mathcal{S}_1 - \mathcal{S}_2|,
\end{aligned} \tag{8}$$

where $k_1 = (\frac{K\mathcal{I}}{1+\beta\mathcal{I}} + d_0)$. Additionally, using the same technique, we have

$$|h_2(t, \mathcal{S}, \mathcal{I}_1, \mathcal{T}, \mathcal{R}) - h_2(t, \mathcal{S}, \mathcal{I}_2, \mathcal{T}, \mathcal{R})| < k_2|\mathcal{I}_1 - \mathcal{I}_2|,$$

$$|h_3(t, \mathcal{S}, \mathcal{I}, \mathcal{T} - 1, \mathcal{R}) - h_3(t, \mathcal{S}, \mathcal{I}_1, \mathcal{T}_2, \mathcal{R})| < k_3|\mathcal{T}_1 - \mathcal{T}_2|,$$

$$|h_4(t, \mathcal{S}, \mathcal{I}, \mathcal{T}, \mathcal{R}_1) - h_4(t, \mathcal{S}, \mathcal{I}_1, \mathcal{T}, \mathcal{R}_2)| < k_4|\mathcal{R}_1 - \mathcal{R}_2|,$$

where

$$\begin{aligned}
k_2 &= \frac{K\mathcal{I}}{(1+\beta\mathcal{I}_2)(1+\beta\mathcal{I}_1)},\\
k_3 &= r + d_0,\\
k_4 &= d_0.
\end{aligned} \tag{9}$$

Therefore, the uniqueness and existence of model (1) indicate that it contains a unique set of solutions.

2.1. Equilibrium points

We identified two types of equilibrium points for our model (1): the disease-free equilibrium (DFE) point and the endemic equilibrium point (EEP).

DFEP:

In model (1), the equilibrium point that corresponds to the absence of eye infection as,

$$E_0(\mathcal{S}, \mathcal{I}, \mathcal{T}, \mathcal{R}) = \left(\frac{b}{d_0}, 0, 0, 0\right). \tag{10}$$

Endemic Equilibrium point EEP:
The endemic equilibrium point is define as, the situation in which eye infection are present in the population, We find the EEP, $E^* = (\mathcal{S}^*, \mathcal{I}^*, \mathcal{T}^*, \mathcal{R}^*)$ are,

$$\begin{aligned}
\mathcal{S}^*(t) &= \frac{\alpha+\mu+d_0}{K}\left[1+\frac{\beta d_0(\mathcal{R}_0-1)}{K+d_0\beta}\right],\\
\mathcal{I}^*(t) &= \frac{d_0(\mathcal{R}_0-1)}{K+d_0\beta},\\
\mathcal{T}^*(t) &= \frac{\mu}{d_0+r}\left[\frac{d_0(\mathcal{R}_0-1)}{K+d_0\beta}\right],\\
\mathcal{R}^*(t) &= \frac{(\mathcal{R}_0-1)}{K+d_0\beta}\left[\alpha+\frac{r\mu}{d_0+r}\right].
\end{aligned} \tag{11}$$

2.2. Expression for $\mathcal{R}_0$

Epidemiology uses the fundamental threshold number, or $\mathcal{R}_0$, to explain how illnesses spread and are treated. We can determine whether the eye disease is spreading through the neighborhood and the most effective strategies to shield the local populace from this dangerous infection by examining $\mathcal{R}_0$. As seen below, $\mathcal{R}_0$ is found using the next-generation method. let $\Phi = (\mathcal{S}, \mathcal{I})$,from the model (1),

$$\frac{d\oplus}{dt} = \mathbb{F} - \mathbb{V},$$

where

$$\mathbb{F} = \begin{pmatrix} \frac{K\mathcal{S}\mathcal{I}}{1+\beta\mathcal{I}} \\ 0 \end{pmatrix}$$

and

$$\mathbb{V} = \begin{pmatrix} -b + d_0\mathcal{S} \\ (\alpha+d_0+\mu)\mathcal{I} \end{pmatrix}.$$

$\mathbb{F}$'s Jacobian for the disease-free state is

$$\mathcal{D}\mathbb{F}(E^0) = \begin{pmatrix} 0 & KS^0 \\ 0 & 0 \end{pmatrix}$$

and $\mathbb{V}$'s Jacobian for the disease-free state is

$$\mathcal{D}\mathbb{V}(E^0) = \begin{pmatrix} d_0 & 0 \\ 0 & \alpha+\mu+d_0 \end{pmatrix}$$

Hence

$$\mathcal{R}_0 = \mathbb{F}\mathbb{V}^{-1} = \frac{Kb}{d_0(\alpha+\mu+d_0)}. \tag{12}$$

Here, on the basic reproduction number $\mathcal{R}_0$, we established the following result.

3. Stability Analysis

In this section, we analyze the local stability of the system (1). To derive the necessary results using the Jacobian matrix, we present the following theorem.

Theorem 1. *The eye infection model (1) is locally asymptotically stable, if* $\mathcal{R}_0 < 1$.

Proof. Jacobian Matrix of eye infection system (1) as,

$$\mathcal{J}^0 = \begin{bmatrix} -d_0 & -K\frac{b}{d_0} & 0 & 0 \\ 0 & K\frac{b}{d_0} - (\alpha+\mu+d_0) & 0 & 0 \\ 0 & \mu & -(r+d_0) & 0 \\ 0 & \alpha & r & -d_0 \end{bmatrix},$$

and

$$|\lambda - \mathcal{J}^0(\mathcal{Q})| = 0.$$

Hence

$$\begin{aligned} \lambda_1 &= -d_0, \\ \lambda_2 &= -(r+d_0), \\ \lambda_3 &= -d_0, \end{aligned}$$

and

$$\begin{aligned} \lambda_4 &= \frac{Kb}{d_0} - (\alpha+\mu+d_0), \\ &= \frac{1}{(\alpha+\mu+d_0)}\left(\frac{Kb}{d_0((\alpha+\mu+d_0))} - 1\right), \\ &= \frac{1}{(\alpha+\mu+d_0)}(\mathcal{R}_0 - 1) \end{aligned}$$

,

Hence, if $(\mathcal{R}_0 - 1) < 0$ then λ_4 is negative and remaining eigenvalues of $\mathcal{J}^0$ are negative, therefore the eye infection model (1) is locally asymptotically stable.

4. Sensitivity Analysis of $\mathcal{R}_0$

Sensitivity analysis is used to evaluate the relative effects of several parameters on model stability, particularly when dealing with ambiguous data. This study also aids in determining the important process factors.
Given that the fundamental reproduction number is

$$\mathcal{R}_0 = \mathbb{F}\mathbb{V}^{-1} = \frac{Kb}{d_0(\alpha+\mu+d_0)}.$$

Parameters	Sensitivity Index
$f(K)$	1
$f(b)$	1
$f(d_0)$	-0.9674
$f(\alpha)$	-0.0124
$f(\mu)$	-0.0124

Table 2: Sensitivity indices of $\mathcal{R}_0$ with respect to model parameters.) .

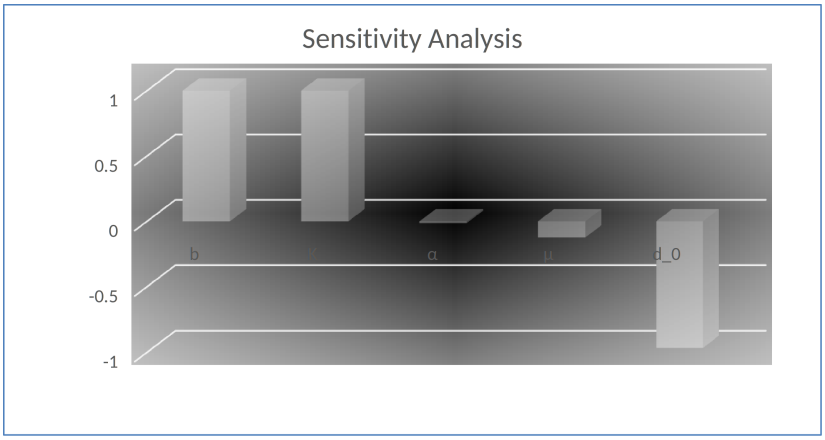

Figure 3: $\mathcal{R}_0$ sensitivity indices relative to model (1) parameters.

We can investigate the sensitivity of $\mathcal{R}_0$ by calculating the partial differentiation of the threshold with regard to the relevant parameters.

$f[y] = \frac{y}{\mathcal{R}_0}\frac{\partial \mathcal{R}_0}{\partial y}$,

(2) The study indicates that the parameters d_0, α, μ, K and b experience contraction and expansion, respectively, and that the value of $\mathcal{R}_0$ is highly responsive to parameter variations. Therefore, for effective infection control, prevention should take precedence over treatment. The aforementioned indices are useful in defining the factors that are essential in defining the infection's capacity for propagation.

5. Numerical Analysis for the Deterministic Model

In this section, we use numerical simulations to confirm the qualitative analysis of model (1). We used non-standard finite difference scheme (NSFD) [24, 25] for simulation. The model's first equation (1) is rewritten with a difference as

$$\frac{d\mathcal{S}}{dt} = b - \frac{K\mathcal{S}\mathcal{I}}{1+\beta\mathcal{I}} - d_0\mathcal{S}. \tag{13}$$

By using the none-standard finite difference method, we decomposed as

$$\frac{\mathcal{S}_{j+1} - \mathcal{S}_j}{h} = b - \frac{K\mathcal{S}_j\mathcal{I}_j}{1+\beta\mathcal{I}_j} - d_0\mathcal{S}_j, \tag{14}$$

Parameters	Numerical value
$\mathcal{S}$	10,12,14
$\mathcal{I}$	0.080000, 0.086000,0.07500
$\mathcal{T}$	0.00500, 0.00600,0.00700
$\mathcal{R}$	0.000200,0.000300,0.000400
b	0.004215
K	0.02
β	0.0039
α	0.008
μ	0.003
d_0	0.01
r	0.0038

Table 3: The system's parameters are explained and given, along with their approximated real values (1).

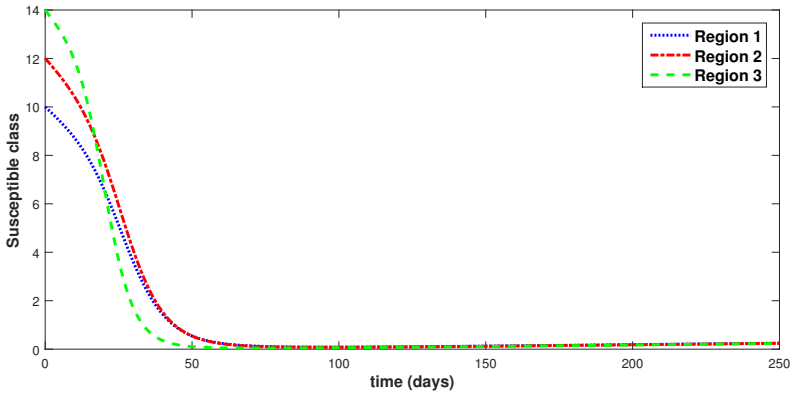

Figure 4: Numerical interpretation of susceptible class of the proposed model.

Like (14), we decomposed the system (1) by using NSFD method

$$\mathcal{S}_{(j+1)} = \mathcal{S}_j + h\left(b - \frac{K\mathcal{S}_j\mathcal{I}_j}{1+\beta\mathcal{I}_j} - d_0\mathcal{S}_j\right),$$
$$\mathcal{I}_{(j+1)} = \mathcal{I}_j + h\left(\frac{K\mathcal{S}_j\mathcal{I}_j}{1+\beta\mathcal{I}_j} - (\alpha+\mu+d_0)\mathcal{I}_j\right),$$
$$\mathcal{T}_{(j+1)} = \mathcal{T}_j + h\left(\mu\mathcal{I}_j - (r+d_0)\mathcal{T}_j\right),$$
$$\mathcal{R}_{(j+1)} = \mathcal{R}_j + h\left(r\mathcal{T}_j + \alpha\mathcal{I}_j - d_0\mathcal{R}_j.\right).$$

We simulate the system (1) using the NSFD technique and the numerical values from [4] that are provided in Table 3. Here in figures 4-7, we use Table 3's numerical values to simulate the outcomes.

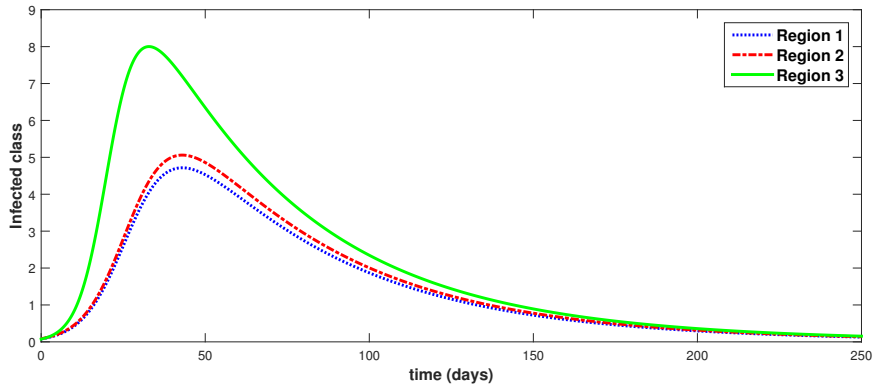

Figure 5: Numerical interpretation of infected class of the proposed model.

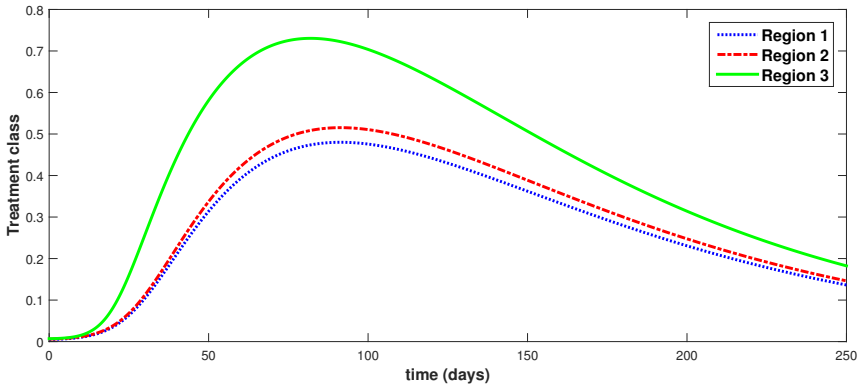

Figure 6: Numerical interpretation of treatment class of the proposed model

6. The stochastic form of the model (1)

In this section, we incorporate the effect of atmospheric white noise by transforming the original deterministic eye disease system (1) into a stochastic system, as described in [26]. To achieve this, nonlinear perturbations are introduced into each equation of the system. Specifically, the rate of change is modified individually for each compartment to reflect the impact of stochastic fluctuations within that class.

$$\begin{aligned}
\mathcal{S}(t): \quad -\beta &\longrightarrow -\beta + (\Phi_{11}S + \Phi_{12})\mathcal{C}_1(t),\\
\mathcal{I}(t): \quad -\mu &\longrightarrow -\mu + (\Phi_{21}S + \Phi_{22})\mathcal{C}_2(t),\\
\mathcal{T}(t): \quad -r &\longrightarrow -r + (\Phi_{31}S + \Phi_{32})\mathcal{C}_3(t),\\
\mathcal{R}(t): \quad -d_0 &\longrightarrow -d_0 + (\Phi_{41}S + \Phi_{42})\mathcal{C}_4(t).
\end{aligned}$$

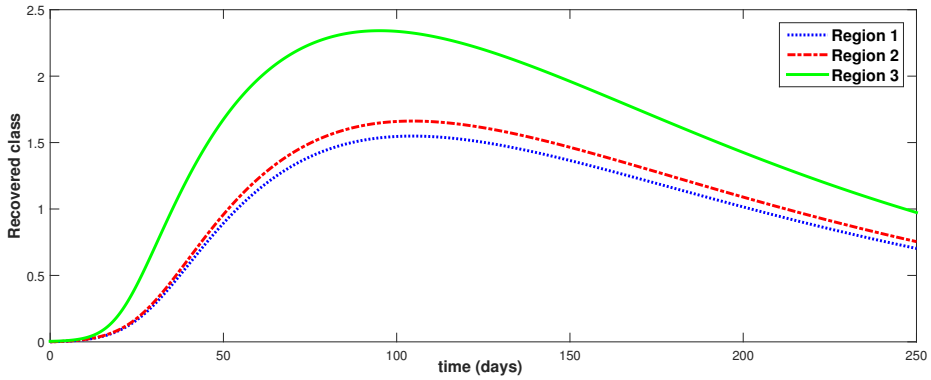

Figure 7: Numerical interpretation of recovered class of the proposed model

The following set of equations represents the stochastic form of system (1):

$$\begin{aligned} d\mathcal{S} &= [b - \tfrac{K\mathcal{S}\mathcal{I}}{1+\beta\mathcal{I}} - d_0\mathcal{S}]dt + (\Phi_{11}\mathcal{S} + \Phi_{12})\mathcal{S}\ d\mathcal{C}_1(t), \\ d\mathcal{I} &= [\tfrac{K\mathcal{S}\mathcal{I}}{1+\beta\mathcal{I}} - (\alpha + \mu + d_0)\mathcal{I}]dt + (\Phi_{21}\mathcal{I} + \Phi_{22})\mathcal{I}\ d\mathcal{C}_2(t), \\ d\mathcal{T} &= [\mu\mathcal{I} - (r + d_0)\mathcal{T}]dt + (\Phi_{31}\mathcal{T} + \Phi_{32})\mathcal{T}\ d\mathcal{C}_3(t), \\ d\mathcal{R} &= [r\mathcal{T} + \alpha\mathcal{I} - d_0\mathcal{R}]dt + (\Phi_{41}\mathcal{R} + \Phi_{42})\mathcal{R}\ d\mathcal{C}_4(t). \end{aligned} \tag{15}$$

6.1. Existence and Uniqueness of Solutions of (15)

Here, we examine and demonstrate the existence and uniqueness of the solutions for the stochastic model (15). First, we established

$$\begin{aligned} d\mathcal{S} &= M_1(t,\mathcal{S},\mathcal{I},\mathcal{T},\mathcal{R})dt + N_1(t,\mathcal{S})d\mathcal{C}_1 t, \\ d\mathcal{I} &= M_2(t,\mathcal{S},\mathcal{I},\mathcal{T},\mathcal{R})dt + N_2(t,\mathcal{S})d\mathcal{C}_2 t, \\ d\mathcal{T} &= M_3(t,\mathcal{S},\mathcal{I},\mathcal{T},\mathcal{R})dt + N_3(t,\mathcal{S})d\mathcal{C}_3 t, \\ d\mathcal{R} &= M_4(t,\mathcal{S},\mathcal{I},\mathcal{T},\mathcal{R})dt + N_4(t,\mathcal{S})d\mathcal{C}_4 t, \end{aligned}$$

secondly, transfer system (15) into a Volterra integral form, as given;

$$\begin{aligned} \mathcal{S}(t) &= \mathcal{S}(0) + \int_0^t M_1(\chi,\mathcal{S},\mathcal{I},\mathcal{T},\mathcal{R})d\chi + \int_0^t N_1(\chi,S)d\mathcal{C}_1(\chi), \\ \mathcal{I}(t) &= \mathcal{I}(0) + \int_0^t M_2(\chi,\mathcal{S},\mathcal{I},\mathcal{T},\mathcal{R})d\chi + \int_0^t N_2(\chi,E)d\mathcal{C}_2(\chi), \\ \mathcal{T}(t) &= \mathcal{T}(0) + \int_0^t M_3(\chi,\mathcal{S},\mathcal{I},\mathcal{T},\mathcal{R})d\chi + \int_0^t N_3(\chi,I)d\mathcal{C}_3(\chi), \\ \mathcal{R}(t) &= \mathcal{R}(0) + \int_0^t M_4(\chi,\mathcal{S},\mathcal{I},\mathcal{T},\mathcal{R})d\chi + \int_0^t N_4(\chi,R)d\mathcal{C}_4(\chi). \end{aligned} \tag{16}$$

To show the existence and uniqueness of the solutions to the eye infection model, we use the following theorem.

Theorem 2. *Suppose, there exist* $\mathcal{K}_i$, $\hat{\mathcal{K}}_i$ *so that there are the following necessary conditions:*

(i) $|M_i(y,t) - M_i(y_i,t)|^2 < \mathcal{K}_i|y-y_i|^2, \quad |N_i(y,t) - N_i(y_i,t)|^2 < \hat{\mathcal{K}}_i|y-y_i|^2,$

(ii) $\forall (y,t) \in \mathbb{R}^4 \times [0,\mathcal{T}]$, *then* $|M_i(y,t)|^2, \quad |N_i(y,t)|^2 < \mathcal{K}(|y|^2+1),$

hold for $i = 1, \cdots, 4$.

We confirm that our model satisfies criteria (i) and (ii) in the Hypothesis. For the susceptible population, we first examine the functions $M_1(t,\mathcal{S},\mathcal{I},\mathcal{T},\mathcal{R})$ and $N_1(t,\mathcal{S})$. We demonstrate the function M's proof using $M(t,\mathcal{S})$.

Proof. First, we look into the functions for the susceptible population, $M_1(t,\mathcal{S},\mathcal{I},\mathcal{T},\mathcal{R})$ and $N_1(t,\mathcal{S})$. Using $M(t,\mathcal{S})$, we demonstrate the proof for the function M.

$$|M_1(t,\mathcal{S}) - M_1(t,\mathcal{S}_1)|^2 = \left|\left(\frac{K\mathcal{I}}{1+\beta\mathcal{I}} + d_0\right)(\mathcal{S}-\mathcal{S}_1)\right|^2. \tag{17}$$

Applying the following norm's definition

$$||\chi||_\infty = \sup_{t\in[0,\mathcal{T}]} |\chi|^2$$

equation (17) is convert to

$$\begin{aligned}
|M_1(t,S) - M_1(t,S_1)|^2 \leq & \sup_{t\in[0,T]} \left|(\frac{K\mathcal{I}}{1+\beta\mathcal{I}} + d_0)(\mathcal{S}-\mathcal{S}_1)\right|^2, \\
\leq & ||(\tfrac{K\mathcal{I}}{1+\beta\mathcal{I}} + d_0)||_\infty^2 |(\mathcal{S}-\mathcal{S}_1)|^2, \\
\leq & \mathcal{K}_1|(\mathcal{S}-\mathcal{S}_1)|^2,
\end{aligned}$$

and

$$\begin{aligned}
|N_1(\mathcal{S},t) - N_1(\mathcal{S}_1,t)|^2 = & |(\Phi_{11}\mathcal{S}+\Phi_{12})\mathcal{S} - (\Phi_{11}\mathcal{S}_1+\Phi_{12})\mathcal{S}_1|^2, \\
\leq & |(\Phi_{11}(\mathcal{S}^2-\mathcal{S}_1^2) - \Phi_{12}(\mathcal{S}-\mathcal{S}_1)|^2, \\
\leq & \Big(\Phi_{11}(\mathcal{S}+\mathcal{S}_1)+\Phi_{12}\Big)^2|\mathcal{S}-\mathcal{S}_1|^2, \\
\leq & \Big(\Phi_{11}^2(\mathcal{S}+\mathcal{S}_1)^2 + 2\Phi_{11}\Phi_{12}(\mathcal{S}+\mathcal{S}_1) + \Phi_{12}^2\Big)|\mathcal{S}-\mathcal{S}_1|^2, \\
\leq & \Big(\Phi_{11}^2(\mathcal{S}^2+2\mathcal{S}\mathcal{S}_1+\mathcal{S}_1^2) + 2\Phi_{11}\Phi_{12}(\mathcal{S}+\mathcal{S}_1) + \Phi_{12}^2\Big)|\mathcal{S}-\mathcal{S}_1|^2, \\
\leq & \Bigg(\sup_{t\in[0,\mathcal{T}]}|\mathcal{S}^2(t)| + 2\sup_{t\in[0,\mathcal{T}]}|\mathcal{S}(t)|\sup_{t\in[0,\mathcal{T}]}|\mathcal{S}_1(t)| + \sup_{t\in[0,\mathcal{T}]}|\mathcal{S}_1^t(t)| \\
& +2\Phi_{11}\Phi_{12}(\sup_{t\in[0,\mathcal{T}]}|\mathcal{S}(t)| + \sup_{t\in[0,\mathcal{T}]}|\mathcal{S}_1(t)|) + \Phi_{12}^2\Bigg)|\mathcal{S}-\mathcal{S}_1|^2, \\
\leq & \Bigg(\Phi_{11}^2\Big(||\mathcal{S}^2||_\infty + 2||\mathcal{S}||_\infty||\mathcal{S}_1||_\infty + ||\mathcal{S}_1^2||_\infty\Big) \\
& +2\Phi_{11}\Phi_{12}||\mathcal{S}||_\infty||\mathcal{S}_1||_\infty + \Phi_{12}^2\Bigg)|\mathcal{S}-\mathcal{S}_1|^2, \\
\leq & \tilde{\mathcal{K}}_1|\mathcal{S}-\mathcal{S}_1|^2
\end{aligned} \tag{18}$$

in which

$$\begin{aligned}\tilde{\mathcal{K}}_1 = &\ \Phi_{11}^2\Big(||\mathcal{S}^2||_\infty + 2||\mathcal{S}||_\infty||\mathcal{S}_1||_\infty + ||\mathcal{S}_1^2||_\infty\Big) + 2\Phi_{11}\Phi_{12}||\mathcal{S}||_\infty||\mathcal{S}_1||_\infty + \Phi_{12}^2,\\ = &\ \Phi_{11}^2\Big(||\mathcal{S}||_\infty + ||\mathcal{S}_1||_\infty||\Big)^2 + 2\Phi_{11}\Phi_{12}||\mathcal{S}||_\infty||\mathcal{S}_1||_\infty|| + \Phi_{12}^2.\end{aligned}$$

Likewise, we can demonstrate that the remaining model equations (15) meet Theorem's condition (i). Consequently,

$$\begin{aligned}\hat{\mathcal{K}}_2 = &\ \Phi_{21}^2\Big(||\mathcal{I}||_\infty + ||\mathcal{I}_1||_\infty||\Big)^2 + 2\Phi_{21}\Phi_{22}||\mathcal{I}||_\infty||\mathcal{I}_1||_\infty + \Phi_{22}^2,\\ \hat{\mathcal{K}}_3 = &\ \Phi_{31}^2\Big(||\mathcal{T}||_\infty + ||\mathcal{T}_1||_\infty||\Big)^2 + 2\Phi_{31}\Phi_{32}||\mathcal{T}||_\infty||\mathcal{T}_1||_\infty + \Phi_{32}^2,\\ \hat{\mathcal{K}}_4 = &\ \Phi_{41}^2\Big(||\mathcal{R}||_\infty + ||\mathcal{R}_1||_\infty||\Big)^2 + 2\Phi_{41}\Phi_{42}||\mathcal{R}||_\infty||\mathcal{R}_1||_\infty + \Phi_{42}^2.\end{aligned}$$

Moreover, we take into account the $\mathcal{I}$ compartment and get

$$\begin{aligned}|M_2(\mathcal{I},t) - M_2(\mathcal{I}_1,t)|^2 = &\ |-(\alpha+\mu+d_0)(\mathcal{I}-\mathcal{I}_1)|^2,\\ \leq &\ 2|(\alpha+\mu+d_0)|^2|(\mathcal{I}-\mathcal{I}_1)|^2,\\ \leq &\ \mathcal{K}_2|(\mathcal{I}-\mathcal{I}_1)|^2\end{aligned}$$

where $\mathcal{K}_2 = 2|(\alpha+\mu+d_0)|^2$. Also, for the $\mathcal{T}$ class, we have that

$$\begin{aligned}|M_3(\mathcal{T},t) - M_3(T_1,t)|^2 = &\ |-(r+d_0)(\mathcal{I}-\mathcal{I}_1)|^2,\\ \leq &\ 2|r+d_0|^2|\mathcal{I}-\mathcal{I}_1|^2,\\ \leq &\ \mathcal{K}_3|\mathcal{I}-\mathcal{I}_1|^2,\end{aligned}$$

where $\mathcal{K}_3 = 2|r+d_0|^2$. Likewise, we have

$$\begin{aligned}|M_4(\mathcal{R},t) - M_4(\mathcal{R}_1,t)|^2 = &\ |-d_0(\mathcal{R}-\mathcal{R}_1)|^2,\\ \leq &\ 2|d_0|\mathcal{R}-\mathcal{R}_1|^2,\\ \leq &\ \mathcal{K}_4|\mathcal{R}-\mathcal{R}_1|^2,\end{aligned}$$

where $\mathcal{K}_4 = 2|d_0|^2$. Then, for our model (15), we prove that conditions (ii) are satisfied.

$$\begin{aligned}|M_1(\mathcal{S},t)|^2 = &\ \left|b - \frac{K\mathcal{S}\mathcal{I}}{1+\beta\mathcal{I}} - d_0\mathcal{S}\right|^2,\\ \leq &\ \left|b - \frac{K\mathcal{S}\mathcal{I}}{1+\beta\mathcal{I}} - d_0\mathcal{S}\right|^2,\\ \leq &\ |\mathcal{S}|^2\left|b - \frac{K\mathcal{I}}{1+\beta\mathcal{I}} - d_0\right|^2,\\ \leq &\ (|\mathcal{S}|^2+1)\left|b - \frac{K\mathcal{I}}{1+\beta\mathcal{I}} - d_0\right|^2,\\ \leq &\ (|\mathcal{S}|^2+1)\sup_{t\in[0,\mathcal{T}]}\left|b - \frac{K\mathcal{I}}{1+\beta\mathcal{I}} - d_0\right|^2,\\ \leq &\ \mathcal{K}^1(|\mathcal{S}|^2+1)\end{aligned}$$

for $\mathcal{K}^1 = \sup_{t\in[0,\mathcal{T}]} \left| b - \frac{K\mathcal{I}}{1+\beta\mathcal{I}} - d_0 \right|^2$.
Also,

$$\begin{aligned} |N_1(\mathcal{S},t) - N_1(\mathcal{S}_1,t)|^2 = & |(\Phi_{11}\mathcal{S}+\Phi_{12})\mathcal{S}|^2, \\ \leq & |\Phi_{11}\mathcal{S}^2+\Phi_{12}\mathcal{S}^2|^2, \\ \leq & \Big(\Phi_{11}+\Phi_{12}\Big)^2|\mathcal{S}^2|^2, \\ \leq & \big(\Phi_{11}+\Phi_{12}\big)^2 \sup_{t\in[0,\mathcal{T}]} |\mathcal{S}^2||\mathcal{S}|^2, \\ \leq & \Big(\Phi_{11}+\Phi_{12}\Big)^2 ||\mathcal{S}^2||_\infty(|\mathcal{S}|^2+1), \\ \leq & \hat{\mathcal{K}}^1(|\mathcal{S}|^2+1), \end{aligned} \tag{19}$$

in which $\hat{\mathcal{K}}^1 = \Big(\Phi_{11}+\Phi_{12}\Big)^2||\mathcal{S}^2||_\infty$. In similar fashion

$$\hat{\mathcal{K}}^2 = \Big(\Phi_{21}+\Phi_{22}\Big)^2||\mathcal{I}^2||_\infty,\ \hat{\mathcal{K}}^3 = \Big(\Phi_{31}+\Phi_{32}\Big)^2||\mathcal{T}^2||_\infty,\ \text{and}\ \hat{\mathcal{K}}^4 = \Big(\Phi_{41}+\Phi_{42}\Big)^2||\mathcal{R}^2||_\infty.$$

Furthermore, we have that for the $\mathcal{I},\mathcal{T}$, and $\mathcal{R}$ compartments,

$$\begin{aligned} |N_2(\mathcal{I},t)|^2 = & \left| \frac{K\mathcal{S}\mathcal{I}}{1+\beta\mathcal{I}} - (\alpha+\mu+d_0)\mathcal{I} \right|^2, \\ \leq & \left| \frac{K\mathcal{S}}{1+\beta} - (\alpha+\mu+d_0) \right|^2 |\mathcal{I}|^2, \\ \leq & (|\mathcal{I}|^2+1) \sup_{t\in[0,\mathcal{T}]} \left| \frac{K\mathcal{S}}{1+\beta} - (\alpha+\mu+d_0) \right|^2, \\ \leq & \mathcal{K}^2(|\mathcal{I}|^2+1), \end{aligned}$$

$$\begin{aligned} |N_3(\mathcal{T},t)|^2 = & |\mu\mathcal{I} - (r+d_0)\mathcal{T}|^2, \\ \leq & |\mu\mathcal{I} - (r+d_0)|^2|\mathcal{T}|^2, \\ \leq & (|\mathcal{T}|^2+1) \sup_{t\in[0,\mathcal{T}]} |\mu\mathcal{I} - (r+d_0)|^2, \\ \leq & \mathcal{K}^3(|\mathcal{T}|^2+1), \end{aligned}$$

$$\begin{aligned} |N_4(\mathcal{R},t)|^2 = & |r\mathcal{T} + \alpha\mathcal{I} - d_0\mathcal{R}|^2, \\ \leq & |r\mathcal{T} + \alpha\mathcal{I} - d_0|^2|\mathcal{R}|^2, \\ \leq & (|\mathcal{R}|^2+1) \sup_{t\in[0,\mathcal{T}]} ||r\mathcal{T} + \alpha\mathcal{I} - d_0|^2, \\ \leq & \mathcal{K}^4(|R|^2+1) \end{aligned}$$

where $\hat{\mathcal{K}}^2 = \sup_{t\in[0,\mathcal{T}]} \left| \frac{K\mathcal{S}}{1+\beta} - (\alpha+\mu+d_0) \right|^2$, $\hat{\mathcal{K}}^3 = \sup_{t\in[0,\mathcal{T}]} |\mu\mathcal{I} - (r+d_0)|^2$, and $\hat{\mathcal{K}}^4 = \sup_{t\in[0,\mathcal{T}]} |r\mathcal{T} + \alpha\mathcal{I} - d_0|^2$.

When every M_i and N_i for $i = 1, 2, \cdots, 4$ meet all the requirements listed in Theorem 2, system (15) existing and has a unique solution. The proof is now complete.

7. The stochastic model's basic reproduction number

The infected compartment $\mathcal{I}$ of the stochastic system (15) is taken into consideration, such that the stochastic fundamental reproduction number can be calculated.

$$d\mathcal{I} = \left[\frac{K\mathcal{S}\mathcal{I}}{1+\beta\mathcal{I}} - (\alpha+\mu+d_0)\mathcal{I}\right]dt + (\Phi_{21}\mathcal{I}+\Phi_{22})\mathcal{I}\ d\mathcal{C}_2(t).$$

Now, utilizing the Ito$'$s formula, we calculate our basic reproduction number stochastically. The Taylor series representing $h(t,\mathcal{I}(t)) = In(\mathcal{I}(t))$ will now be examined.

$$dh(t,\mathcal{I}(t)) = \frac{\partial h}{\partial t}dt + \frac{\partial h}{\partial \mathcal{I}(t)}d\mathcal{I}(t) + \frac{1}{2}\frac{\partial^2 h}{\partial \mathcal{I}^2(t)}(d\mathcal{I}(t))^2 + \frac{\partial^2 h}{\partial \mathcal{I}(t)\partial t}d\mathcal{I}(t)dt + \frac{1}{2}\frac{\partial^2 h}{\partial t^2}(dt)^2.$$

Where $\frac{\partial h}{\partial t} = 0$, $\frac{\partial h}{\partial \mathcal{I}(t)} = \frac{1}{\mathcal{I}(t)}$, $\frac{\partial^2 h}{\partial \mathcal{I}^2(t)} = \frac{1}{\mathcal{I}^2(t)}$, $\frac{\partial^2 h}{\partial \mathcal{I}\partial t} = 0$ and $\frac{\partial^2 h}{\partial t^2} = 0$

$$dh(t,\mathcal{I}(t)) = \frac{1}{\mathcal{I}(t)}d\mathcal{I}(t) - \frac{1}{2\mathcal{I}^2(t)}d\mathcal{I}^2(t).$$

This implies,

$$dh(t,\mathcal{I}(t)) = \frac{1}{\mathcal{I}(t)}\left[(\frac{K\mathcal{S}\mathcal{I}}{1+\beta\mathcal{I}} - (\alpha+\mu+d_0)\mathcal{I})dt + (\Phi_{21}\mathcal{I}+\Phi_{22})\mathcal{I}\ d\mathcal{C}_2(t)\right]$$
$$-\frac{1}{2\mathcal{I}^2(t)}\left([\frac{K\mathcal{S}\mathcal{I}}{1+\beta\mathcal{I}} - (\alpha+\mu+d_0)\mathcal{I}]dt + (\Phi_{21}\mathcal{I}+\Phi_{22})\mathcal{I}\ d\mathcal{C}_2(t)\right)^2(t).$$

Then, applying the chain law, we get

$$dh(t,\mathcal{I}(t)) = \left[\frac{K\mathcal{S}\mathcal{I}}{1+\beta\mathcal{I}} - (\alpha+\mu+d_0)\mathcal{I} - \frac{1}{2}(\Phi_{21}\mathcal{I}+\Phi_{22})^2\right]dt + (\Phi_{21}\mathcal{I}+\Phi_{22})d\mathcal{C}_2(t).$$

Assume that the current infection opening rate is $\mathbb{F}$ and the new virus transfer rate is $\mathbb{V}$. Following that, E_0 and $\mathbb{F}$ at the disease-free point of equilibrium turn into,

$$\mathbb{F} = \left[\frac{kb}{d_0} - \frac{1}{2}(\Phi_{21}\mathcal{I}+\Phi_{22})^2\right],$$
$$\mathbb{V} = (\alpha+\mu+d_0),$$
$$\mathbb{V}^{-1} = \frac{1}{(\alpha+\mu+d_0)}.$$

This, implies

$$\mathbb{F}\mathbb{V}^{-1} = \left[\frac{kb}{d_0(\alpha+\mu+d_0)} - \frac{(\Phi_{21}\mathcal{I}+\Phi_{22})^2}{2(\alpha+\mu+d_0)}\right].$$

Where, $\mathcal{R}_1 = \frac{kb}{d_0(\alpha+\mu+d_0)}$ Therefore, our fundamental delta virus reproduction number under the stochastic system is,

$$\mathcal{R}_1^S = \mathcal{R}_1 - \frac{(\Phi_{21}\mathcal{I}+\Phi_{22})^2}{2(\alpha+\mu+d_0)}.$$

8. Stability Analysis of stochastic model

The stable behavior within a stochastic system dependent upon the stochastic fundamental reproduction number is covered in this section. According to the following theory, the stochastic system (15) will be locally asymptotically stable if either $\mathcal{R}_1^S < 1$ or $\mathcal{R}_2^S < 1$.

Theorem 3. *If $\mathcal{R}_1^S < 1$, then E^0 is a locally asymptotically stable DFE point.*

Proof. Given a Taylor expansion such as $F(t, \mathcal{I}(t)) = ln\mathcal{I}(t)$, the $it\hat{0}$ formula yields

$$\begin{aligned} dF(t,\mathcal{I}(t)) &= \left[\frac{K\mathcal{S}\mathcal{I}}{1+\beta\mathcal{I}} - (\alpha+\mu+d_0) - \frac{1}{2}(\Phi_{21}\mathcal{S}+\Phi_{22})^2\right]dt \\ &+ (\Phi_{21}\mathcal{S}+\Phi_{22})d\mathcal{C}_3(t), \end{aligned}$$

$$\begin{aligned} dln\mathcal{I}(t) &= \left[\frac{K\mathcal{S}\mathcal{I}}{1+\beta\mathcal{I}} - (\alpha+\mu+d_0) - \frac{1}{2}(\Phi_{21}\mathcal{S}+\Phi_{22})^2\right]dt \\ &+ (\Phi_{21}\mathcal{S}+\Phi_{22})d\mathcal{C}_3(t). \end{aligned} \tag{20}$$

Apply integration on (20), we get

$$\begin{aligned} ln\mathcal{I}(t) - ln\mathcal{I}(0) &= \int_0^t \left(\frac{K\mathcal{S}\mathcal{I}}{1+\beta\mathcal{I}} - (\alpha+\mu+d_0) - \frac{1}{2}(\Phi_{21}\mathcal{S}+\Phi_{22})^2\right)dt \\ &+ \int_0^t (\Phi_{21}\mathcal{S}+\Phi_{22})d\mathcal{C}_3(t). \end{aligned} \tag{21}$$

Now, it DFE equilibrium point solve (21), we get

$$\begin{aligned} ln\mathcal{I}(t) &= ln\mathcal{I}(0) + \int_0^t \left(\frac{Kb}{d_0} - (\alpha+\mu+d_0) - \frac{1}{2}(\Phi_{21}\mathcal{S}+\Phi_{22})^2\right)dt \\ &+ \int_0^t (\Phi_{21}\mathcal{S}+\Phi_{22})d\mathcal{C}_3(t). \end{aligned}$$

$$ln\mathcal{I}(t) \leq ln\mathcal{I}(0) + \left(\frac{Kb}{d_0} - (\alpha+\mu+d_0) - \frac{1}{2}(\Phi_{21}\mathcal{S}+\Phi_{22})^2\right)dt + H(t). \tag{22}$$

Where $H(t) = \int_0^t (\Phi_{21}\mathcal{S}+\Phi_{22})d\mathcal{C}_3(t)$.
We know, that $\lim_{t\to\infty} sup\frac{H(t)}{t} = 0$, using martingales. Furthermore, divide (22) by t and apply $\lim_{t\to\infty} sup$, we get

$$\begin{aligned} \lim_{t\to\infty} sup\frac{ln\mathcal{I}(t)}{t} &\leq \lim_{t\to\infty} sup\left(\frac{Kb}{d_0} - (\alpha+\mu+d_0) - \frac{1}{2}(\Phi_{21}\mathcal{S}+\Phi_{22})^2\right)t \\ &+ \lim_{t\to\infty} sup\frac{H(t)}{t}. \end{aligned} \tag{23}$$

This implies,

$$\begin{aligned}\lim_{t\to\infty} sup\frac{ln\mathcal{I}(t)}{t} &\leq \left(\frac{Kb}{d_0} - (\alpha+\mu+d_0) - \frac{1}{2}(\Phi_{21}\mathcal{S}+\Phi_{22})^2\right)dt < 0.\\ &= (\alpha+\mu+d_0)\left(\frac{Kb}{d_0(\alpha+\mu+d_0)} - \frac{(\Phi_{21}\mathcal{S}+\Phi_{22})^2}{2(\alpha+\mu+d_0)} - 1\right) < 0.\\ &= (\alpha+\mu+d_0)(\mathcal{R}_1^S - 1).\end{aligned}$$

We know $(\alpha+\mu+d_0) > 0$, therefore

$$(\mathcal{R}_1^S - 1) < 0,$$

implies

$$\mathcal{R}_1^S < 1.$$

Therefore, if $\mathcal{R}_1^S < 1$, then the DFE point E_0 is locally asymptotically stable.

9. Numerically analysis of the stochastic model

Using the Euler-Maruyama approach, the trajectories or approximated solutions of a stochastic system problem are found using the following equation:

$$\chi_{t_{i+1}} = \chi_{t_i} + \alpha(t_i, \chi_{t_i}) + \beta(t_i, \chi_{t_i})\Delta A_i. \tag{24}$$

The case where $i = 0, 1, ..., n-1$. Comprehending the computation of ΔA_i is necessary for the computational implementation of the process. instances in which $i = 0, 1, ..., n-1$. The computer implementation of the procedure requires an understanding of how to compute of ΔA_i. Suppose that η is a random variable with an average $\eta \sim M(0,1)$. A normal distribution is thus indicated by $\sqrt{\Delta}t\eta_1$ with zero mean and variance Δt, that is, $\sqrt{\Delta}t\eta_1 \sim M(0, \Delta t)$. The system of dynamic differential equations (15) must be appropriately separated for our suggested model in order to apply the Euler-Maruyama approach method similarly (24). This can be done by

$$\begin{aligned}\mathcal{S}_{t_{i+1}} &= \mathcal{S}_{t_i} + \left[b - \tfrac{K\mathcal{S}\mathcal{I}}{1+\beta\mathcal{I}} - d_0\mathcal{S}\right]\Delta t + \sqrt{\Delta}t\eta_1,\\ \mathcal{I}_{t_{i+1}} &= \mathcal{I}_{t_i} + \left[\tfrac{K\mathcal{S}\mathcal{I}}{1+\beta\mathcal{I}} - (\alpha+\mu+d_0)\mathcal{I}\right]\Delta t + \sqrt{\Delta}t\eta_2,\\ \mathcal{T}_{t_{i+1}} &= \mathcal{T}_{t_i} + [\mu\mathcal{I} - (r+d_0)\mathcal{T}]\Delta t + \sqrt{\Delta}t\eta_3,\\ \mathcal{R}_{t_{i+1}} &= \mathcal{R}_{t_i} + [r\mathcal{T} + \alpha\mathcal{I} - d_0\mathcal{R}]\Delta t + \sqrt{\Delta}t\eta_4.\end{aligned} \tag{25}$$

We consider the initial data as given by $(\mathcal{S}(0), \mathcal{I}(0), \mathcal{T}(0), \mathcal{R}(0)) = (800, 700, 500, 200)$ and use the parameters values given in Table 3 to simulate the results of stochastic model in figure 8. In addition, we compare the deterministic and stochastic model in figures 9-12 respectively of different classes. In the model, the susceptible population gradually decreases as individuals become infected. The number of infected cases initially rises for a

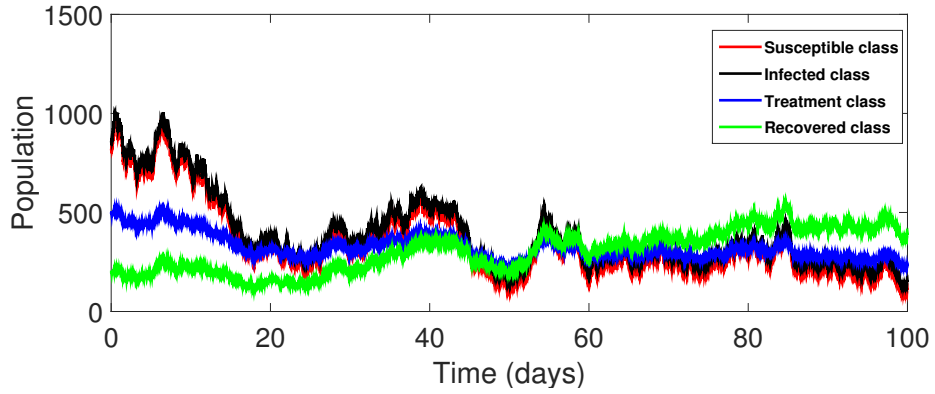

Figure 8: Papulation dynamics of stochastic model (15).

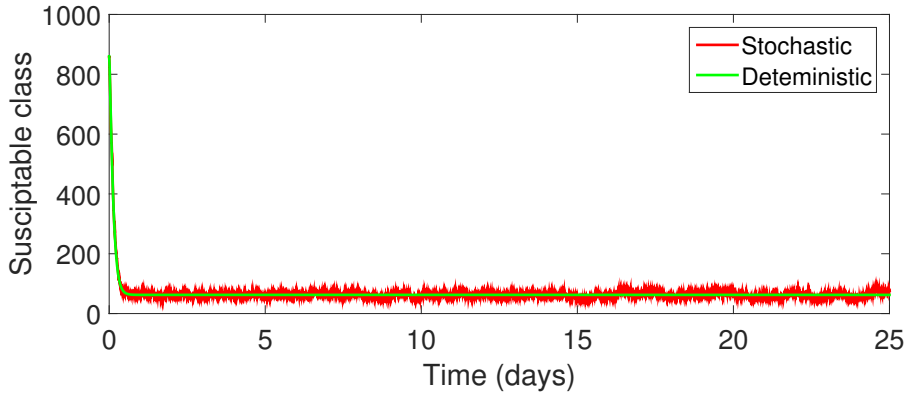

Figure 9: Comparison between deterministic and stochastic numerical interpretation of susceptible class under stochastic type model.

period of time but then begins to decline as treatment is introduced. During this process, some individuals recover naturally without treatment, while others recover after receiving treatment. As a result, the recovered population increases steadily and grows rapidly over time. Furthermore, a comparison between the numerical results of the stochastic and deterministic models shows that both approaches are in close agreement, confirming the reliability of the simulations.

10. Conclusion

In recent years, eye infectious diseases have attracted increasing attention in research, highlighting the need for new mathematical frameworks to study their dynamics from multiple perspectives. In this work, we developed and analyzed a mathematical model of eye infections using both deterministic and stochastic approaches. Key analyses were conducted, including the computation of disease-free and endemic equilibria, as well as the derivation of the basic reproduction numbers for both models. Theoretical results on existence and stability were established using tools from nonlinear analysis. For the

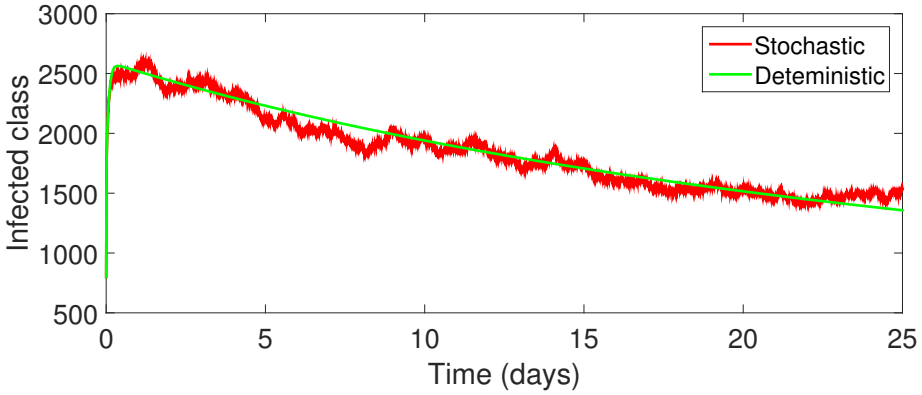

Figure 10: Comparison between deterministic and stochastic numerical interpretation of infected class under stochastic type model.

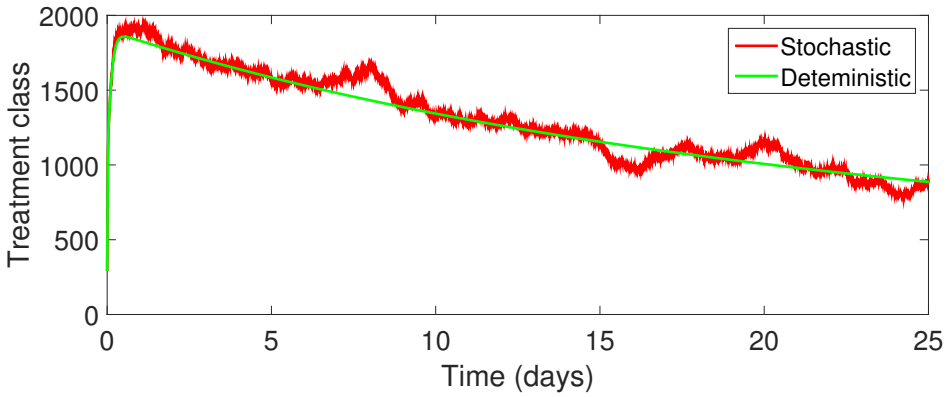

Figure 11: Comparison between deterministic and stochastic numerical interpretation of treatment class under stochastic type model.

deterministic model, a nonstandard finite difference (NSFD) scheme was employed, while for the stochastic model, a robust numerical algorithm was implemented. Numerical simulations and graphical illustrations were provided, and a comparison between the two modeling approaches demonstrated close agreement, thereby validating the accuracy and reliability of the proposed methodology. Overall, this study offers valuable insights into the transmission dynamics of eye infections and provides a solid foundation for future investigations and control strategies.

Acknowledgements

The authors would like to acknowledge the support of Prince Sultan University for paying the Article Processing Charges (APC) of this publication.

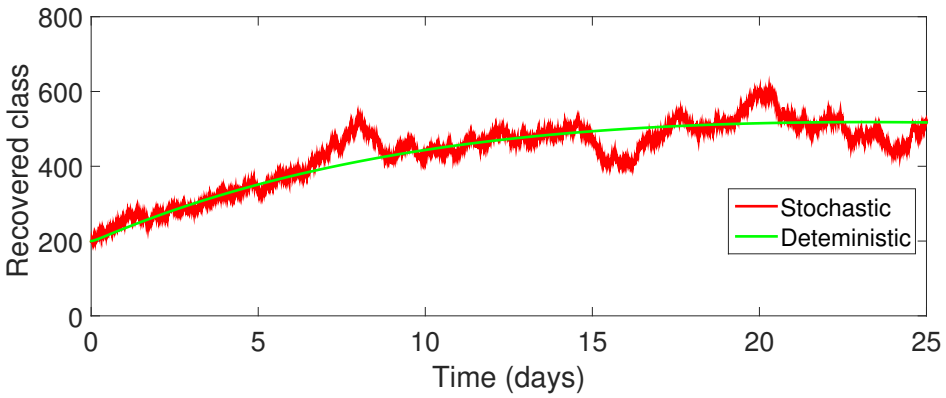

Figure 12: Comparison between deterministic and stochastic numerical interpretation of recovered class under stochastic type model.

References

[1] Ching-Shan Chou and Avner Friedman. Introduction to mathematical biology. 2010.

[2] Edward K Yeargers, James V Herod, and Ronald W Shonkweiler. An introduction to the mathematics of biology: with computer algebra models. 2013.

[3] Kamal Shah, Fahd Jarad, and Thabet Abdeljawad. On a nonlinear fractional order model of dengue fever disease under caputo-fabrizio derivative. *Alexandria Engineering Journal*, 59(4):2305–2313, 2020.

[4] Fazal Haq, Kamal Shah, Ghaus-UR Rahman, and Muhammad Shahzad. Numerical analysis of fractional order model of hiv-1 infection of cd4+ t-cells. *Computational Methods for Differential Equations*, 5(1):1–11, 2017.

[5] Rahim Ud Din, Kamal Shah, Imtiaz Ahmad, and Thabet Abdeljawad. Study of transmission dynamics of novel covid-19 by using mathematical model. *Advances in Difference Equations*, 2020(1):323, 2020.

[6] Willi Jäger and James D Murray. Modelling of patterns in space and time: Proceedings of a workshop held by the sonderforschungsbereich 123 at heidelberg july 4–8, 1983. 55, 2013.

[7] SN Kyere, FA Boateng, GF Hoggar, and P Jonathan. Optimal control model of haemorrhagic conjunctivitis disease. *Adv. Comput. Sci.*, 1(2):108, 2018.

[8] Tracy Lee and Irene C Kuo. Survey of state conjunctivitis policies for school-age students. *Journal of American Association for Pediatric Ophthalmology and Strabismus*, 26(3):115–e1, 2022.

[9] Sasha R Fehily, Gail B Cross, and Andrew J Fuller. Bilateral conjunctivitis in a returned traveller. *PLoS Neglected Tropical Diseases*, 9(1):e0003351, 2015.

[10] Robert H Elliot. Conjunctivitis in the tropics. *British Medical Journal*, 1(3340):12, 1925.

[11]

[12] David W Kimberlin. Red book: 2018-2021 report of the committee on infectious diseases. Number Ed. 31, 2018.

[13] Sireepatch Sangsawang, Tareerat Tanutpanit, Wannissa Mumtong, and Puntani Pongsumpun. Local stability analysis of mathematical model for hemorrhagic conjunctivitis disease. *Current Applied Science and Technology*, 12(2):189–197, 2012.

[14] O Ghazali, KB Chua, KP Ng, PS Hooi, MA Pallansch, MS Oberste, KH Chua, and JW Mak. An outbreak of acute haemorrhagic conjunctivitis in melaka, malaysia. *Singapore Med J*, 44(10):511–6, 2003.

[15] J Chansaenroj, S Vongpunsawad, J Puenpa, A Theamboonlers, V Vuthitanachot, P Chattakul, D Areechokchai, and Y Poovorawan. Epidemic outbreak of acute haemorrhagic conjunctivitis caused by coxsackievirus a24 in thailand, 2014. *Epidemiology & Infection*, 143(14):3087–3093, 2015.

[16] Suratchata Sangthongjeen, Anake Sudchumnong, and Surapol Naowarat. Effect of educationa campaign on tranmission model of conjunctivitis. *Australia Journal of Basis and Applied Science*, 9(7):811–815, 2015.

[17] G Chowell, E Shim, Fred Brauer, P Diaz-Dueñas, JM Hyman, and Carlos Castillo-Chavez. Modelling the transmission dynamics of acute haemorrhagic conjunctivitis: application to the 2003 outbreak in mexico. *Statistics in medicine*, 25(11):1840–1857, 2006.

[18] J Suksawat and Surapol Naowarat. Effect of rainfall on the transmission model of conjunctivitis. 2014.

[19] B Unyong and S Naowarat. Stability analysis of conjunctivitis model with nonlinear incidence term. *Australian Journal of Basic and Applied Sciences*, 8(24):52–58, 2014.

[20] Sireepatch Sangsawang, Tareerat Tanutpanit, Wannissa Mumtong, and Puntani Pongsumpun. Local stability analysis of mathematical model for hemorrhagic conjunctivitis disease. *Current Applied Science and Technology*, 12(2):189–197, 2012.

[21] O Ghazali, KB Chua, KP Ng, PS Hooi, MA Pallansch, MS Oberste, KH Chua, and JW Mak. An outbreak of acute haemorrhagic conjunctivitis in melaka, malaysia. *Singapore Med J*, 44(10):511–6, 2003.

[22] J Chansaenroj, S Vongpunsawad, J Puenpa, A Theamboonlers, V Vuthitanachot, P Chattakul, D Areechokchai, and Y Poovorawan. Epidemic outbreak of acute haemorrhagic conjunctivitis caused by coxsackievirus a24 in thailand, 2014. *Epidemiology & Infection*, 143(14):3087–3093, 2015.

[23] G Chowell, E Shim, Fred Brauer, P Diaz-Dueñas, JM Hyman, and Carlos Castillo-Chavez. Modelling the transmission dynamics of acute haemorrhagic conjunctivitis: application to the 2003 outbreak in mexico. *Statistics in medicine*, 25(11):1840–1857, 2006.

[24] Zhuo-Jia Fu, Zhuo-Chao Tang, Hai-Tao Zhao, Po-Wei Li, and Timon Rabczuk. Numerical solutions of the coupled unsteady nonlinear convection-diffusion equations based on generalized finite difference method. *The European Physical Journal Plus*, 134(6):272, 2019.

[25] Israr Ahmad, Zeeshan Ali, Babar Khan, Kamal Shah, and Thabet Abdeljawad. Exploring the dynamics of gumboro-salmonella co-infection with fractal fractional analysis. *Alexandria Engineering Journal*, 117:472–489, 2025.

[26] Kamal Shah, Khalil Ur Rehman, Bahaaeldin Abdalla, Thabet Abdeljawad, and Wasfi

Shatanawi. Using neural network and fractals fractional analysis to predict the eye disease infection caused by conjunctivitis virus. *Fractals*, page 2540204, 2025.